EVALUATION OF TOPOGRAPHIC CORRECTION MODELS IN MULTISPECTRAL IMAGES ACQUIRED BY UNMANNED AERIAL VEHICLE (UAV)

Isabele Canesin Longo [1], Rebeca Campos Emiliano da Silva [2], Renato César dos Santos[3], Nilton Nobuhiro Imai [4]

[1] Undergraduate Student in Environmental Engineering, Universidade Estadual Paulista (FCT/UNESP), Presidente Prudente, Brazil – isabele.longo@unesp.br
[2] Graduate Program in Cartographic Sciences, Universidade Estadual Paulista (FCT/UNESP), Presidente Prudente, Brazil – rebeca.silva@unesp.br
[3, 4] Department of Cartography, Universidade Estadual Paulista (FCT/UNESP), Presidente Prudente, Brazil – nilton.imai@unesp.br, renato.santos@unesp.br

Keywords: topographic correction, UAV imagery, multispectral sensors, radiometric normalization, environmental monitoring.

Abstract

Topographic effects can introduce radiometric distortions in multispectral images acquired by Unmanned Aerial Vehicles (UAVs), compromising their reliability for environmental and agricultural applications. This study evaluates the performance of six classical topographic correction models: Simple Ratio, Cosine, C Correction, SCS+C, Empirical-Statistical, and Empirical-Rotational, applied to high-resolution UAV imagery. Data collection was conducted using a DJI Mavic 3 Multispectral at an altitude of 75.9 meters over a 0.5-hectare area with irregular relief. A total of 84 multispectral images were acquired and processed. Descriptive statistics (mean, median, and standard deviation) were estimated using ten calibration panels to assess the models. Results demonstrated that C Correction and Empirical-Rotational consistently reduced variability among calibration panels, providing the most effective correction without altering mean reflectance values. In contrast, the Simple Ratio and Empirical-Statistical models increased data dispersion, indicating limited suitability for UAV imagery in complex terrain. These findings emphasize the importance of selecting appropriate topographic correction models to ensure consistent spectral responses, thereby supporting applications such as vegetation monitoring, biomass estimation, and environmental studies.

1. Introduction

The advancement of remote sensing technologies using Unmanned Aerial Vehicles (UAVs) has consolidated these systems as essential tools for acquiring high-resolution multispectral imagery. UAV-based data have been increasingly applied in precision agriculture, land use and land cover monitoring, and environmental studies (Colomina and Molina, 2014; Ma et al., 2013; Rango et al., 2006; Berni et al., 2009). Their high spatial and temporal resolution enhances the capacity to analyze areas of difficult access with efficiency and relatively low cost.

Nevertheless, the spectral response recorded by UAV sensors is influenced by physical and geometric variables, such as solar incidence angle, slope, and terrain aspect. These factors introduce radiometric distortions that compromise the comparability between spectrally similar panels (Blanco et al., 2001; Cao et al., 2019). Radiometric distortions, resulting from the interaction between relief and illumination, are especially pronounced in areas with rugged topography, where slopes and variable orientations create shadowing and non-uniform illumination conditions. To mitigate these effects, topographic correction models are applied to relate apparent reflectance to the geometry of illumination (Teillet, Guindon and Goodenough, 1982; Smith et al., 1980).

Among the classical approaches, the Cosine and C-Correction models have been widely applied to orbital imagery. However, recent studies emphasize the need to evaluate their effectiveness for UAV imagery, where specific conditions, such as low flight altitude and high angular variability, intensify undesired radiometric effects (Honkavaara et al., 2018; Rosas et al., 2020). Assessing the efficiency of topographic correction models is particularly relevant for environmental and agricultural applications. In forest ecosystems, such corrections improve the detection of deforestation and natural regeneration. In agriculture, they enhance the consistency of vegetation indices used to estimate biomass and detect water or nutrient stress. These applications illustrate the importance of minimizing topographic distortions to ensure reliable spectral information (Smith and Milton, 1999; Florenzano, 2008).

In this context, the present study evaluates the performance of classical and empirical topographic correction models applied to UAV-based multispectral imagery. A total of six models were tested: Simple Ratio, Cosine, C Correction, SCS+C, Empirical-Statistical, and Empirical-Rotational. The analysis relied on descriptive statistics (mean, median, and standard deviation) calculated from calibration panels to identify the strengths and limitations of each model under variable topographic conditions.

2. Methodology

2.1 Study Area and Data Acquisition

The study was conducted in an experimental area of approximately 0.5 ha, characterized by irregular relief with altitudinal variations of about 17 meters. Multispectral images were acquired using a DJI Mavic 3 Multispectral (M3M) UAV at an average flight altitude of 80 m, resulting in a ground sampling distance (GSD) of approximately 2.1 cm. The sensor includes five discrete bands: Blue (centered at 450 ± 16 nm), Green (560 ± 16 nm), Red (650 ± 16 nm), Red Edge (730 ± 16 nm), and Near Infrared – NIR (840 ± 26 nm), in addition to an RGB camera for true-color visualization. A total of 84 multispectral images were collected over the study area.

For georeferencing, ten points were measured in the field with a dual-frequency Global Navigation Satellite System (GNSS) receiver. Seven of these points were used as ground control points (GCPs) and three as independent check points. The phototriangulation process resulted in a root mean square error (RMSE) of 8.5 cm for the check points. All data were referenced to the SIRGAS 2000 / UTM Zone 22S coordinate system (EPSG:31982).

2.2 Image Processing

Image processing was performed using Agisoft Metashape Professional v.2.2.1 (Agisoft LLC, St. Petersburg, Russia). The workflow included image alignment, optimization with GCPs, and the generation of a digital elevation model (DEM) and orthomosaics for each spectral band.
Subsequently, the DEM was imported into ArcGIS Pro v.3.2 (Esri, Redlands, USA) to derive slope and aspect maps, expressed in radians, which are required for the application of the topographic correction models.

2.3 Topographic Correction Models

Six correction models (Table 1) were tested. The models are based on the illumination factor (IL), calculated from solar zenith angle (θ_0), solar azimuth (ϕ_0), terrain slope (θn), and aspect (ϕ_n) (Teillet et al., 1982). The following equation is used:

$$IL = cos(\theta_0)cos(\theta n) + sin(\theta_0)sin(\theta n)cos(\phi_0 - \phi_n) \quad (1)$$

Model	Formula	Reference
Simple Ratio Model (SRM)	$L_c = \frac{L_0}{IL}$	Smith et al. (1980)
Cosine Model	$L_c = L_0 \cdot \frac{Cos(\theta_s)}{IL}$	Teillet, Guindon & Goodenough (1982)
C Correction	$L_c = L_0 \cdot \frac{cos\theta_s + c}{IL + c}$	Teillet et al. (1982)
SCS+C	$L_c = L_0 \cdot \frac{cos\theta_s cos\theta_t + c}{IL + c}$	Soenen et al. (2005)
Empirical-Statistical	$L_c = L_0 - m * IL - b + \bar{L}_0$	Teillet et al. (1982)
Empirical-Rotational	$L_c = \bar{L}_0 - m * IL - cos\theta_s$	Tan et al. (2010)

Table 1. Topographic correction models.

Table 2 summarizes the formulas used in each correction model, along with the definitions of the variables and parameters.

Symbol	Meaning	How to Obtain
L_0	Original reflectance (on inclined surface)	Obtained from the image (DN converted to TOA or BOA reflectance)
$\bar{L}_0$	Mean reflectance of the original scene*	Simple average of L_0
θ_s	Solar zenith angle	Obtained using GPS and image timestamp
θ_t	Terrain slope	Derived from DEM
c	Constant in C and SCS+C models	$L_0 = m \cdot IL + b$ $c = \frac{b}{m}$

Table 2. Description of variables.

2.4 Radiometric Quality Assessment

To evaluate the effectiveness of the correction models, ten calibration panels were distributed in the study area (Figure 1). For each panel, polygons were manually delineated on the orthomosaics. From these polygons, descriptive statistics (mean, median, and standard deviation) were extracted for each spectral band and each correction model.

Figure 1. Overview of the study area with the distribution of all calibration panels.

The results were then aggregated per spectral band and correction model. The main criterion for evaluating performance was the reduction of variability among panels, represented by the mean of the standard deviations. A detailed view of three calibration panels is shown in Figure 2, exemplifying the areas used for statistical extraction.

Figure 2. Zoomed view of three calibration panels, illustrating the regions of interest used for statistical analysis.

3. Results

The analysis demonstrated that the performance of the topographic correction models varied across spectral bands (Tables 2–6; Figures 5–7). The evaluation criterion was the reduction of variability among calibration panels, represented by the standard deviation of the panel means. Complementary indicators, such as mean and median values, are also presented to illustrate overall stability.

In the Blue and Green bands (Tables 3–4), the C Correction model achieved the best performance, with standard deviation values close to those of the original image, indicating that it corrected topographic effects without introducing distortions. In contrast, the SRM and Cosine models significantly increased data dispersion, showing limited applicability under the illumination and terrain conditions of the study area.

Model	Mean	Median	Standard deviation
Original	45361,46	45384,00	1201,20
Simple Ratio Model (SRM)	66663,82	66059,87	4058,09
Cosine Model	45778,49	45363,75	2786,72
C Correction	45378,09	45351,54	1200,44
SCS+C	47946,74	47923,85	1267,47
Empirical-Statistical	72006,03	72030,32	2418,27
Empirical-Rotational	44884,48	44891,71	1206,63

Table 3. Mean, median, and standard deviation of panel values for the blue band.

Model	Mean	Median	Standard deviation
Original	46952,34	47073,00	1149,99
Simple Ratio Model (SRM)	68705,69	67923,23	4127,43
Cosine Model	47180,66	46643,34	2834,33
C Correction	47000,68	47111,47	1164,74
SCS+C	46986,36	47098,64	1164,01
Empirical-Statistical	74268,01	74497,26	2339,40
Empirical-Rotational	46435,52	46549,00	1167,61

Table 4. Mean, median, and standard deviation of panel values for the green band.

For the Red band (Table 5), the SCS+C model stood out by providing the lowest standard deviation, strongly reducing variability among panels. Although it produced lower mean reflectance values compared to the original, the model demonstrated high effectiveness in homogenizing spectral responses. C Correction and Empirical-Rotational also maintained mean and median values similar to the original image while reducing variability.

Model	Mean	Median	Standard deviation
Original	46952,34	48205,00	1189,30
Simple Ratio Model (SRM)	71304,10	70247,33	4340,06
Cosine Model	47180,66	48239,32	2980,35
C Correction	48172,85	48182,38	1201,13
SCS+C	12413,88	12435,17	307,74
Empirical-Statistical	79200,95	79375,42	2388,13
Empirical-Rotational	46300,69	46380,60	1190,79

Table 5. Mean, median, and standard deviation of plate values for the red band.

In the Red Edge band (Table 6), both C Correction and SCS+C reduced variability relative to the original image, with SCS+C presenting slightly better performance. Conversely, SRM and Empirical-Statistical showed large increases in dispersion, exceeding 6000 in some cases.

Model	Mean	Median	Standard deviation
Original	47782,37	48123,00	3560,48
Simple Ratio Model (SRM)	69128,72	68817,63	6005,07
Cosine Model	47471,16	47257,53	4123,72
C Correction	47821,81	48158,45	3491,44
SCS+C	44580,12	44896,92	3258,02
Empirical-Statistical	77484,04	78178,39	7015,58
Empirical-Rotational	47263,15	47603,54	3504,42

Table 6. Mean, median, and standard deviation of panel values for the Red Edge band.

Finally, in the NIR band (Table 7), SCS+C achieved the most significant homogenization among calibration panels, with the lowest variability overall. C Correction also reduced dispersion compared to the original, whereas SRM and Empirical-Statistical again produced the highest variability values.

Model	Mean	Median	Standard deviation
Original	47721,77	48165,00	3881,79
Simple Ratio Model (SRM)	69048,99	70261,25	6319,57
Cosine Model	47416,40	48248,88	4339,69
C Correction	47634,46	48103,23	3812,31
SCS+C	12113,57	12225,26	982,91
Empirical-Statistical	79304,53	80180,51	7731,10
Empirical-Rotational	45947,53	46388,98	3852,62

Table 7. Mean, median, and standard deviation of panel values for the Near Infrared (NIR) band.

The overall trends are summarized in Figures 3–5, which illustrate the mean, median, and standard deviation values across all bands and models. The results highlight the superior performance of SCS+C, particularly in the Red and NIR bands, while C Correction consistently provided stable though less pronounced improvements. In contrast, SRM and Empirical-Statistical systematically increased reflectance and variability, confirming their limited suitability for UAV-based multispectral imagery in complex terrain.

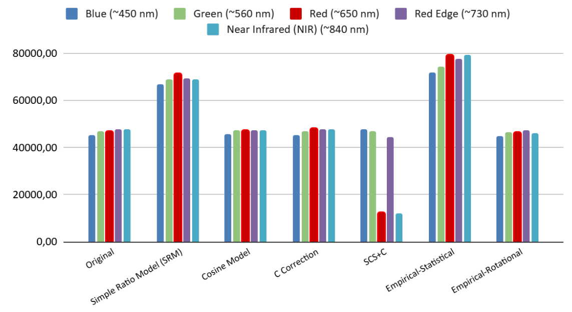

Figure 3. Mean of calibration panels by model and band.

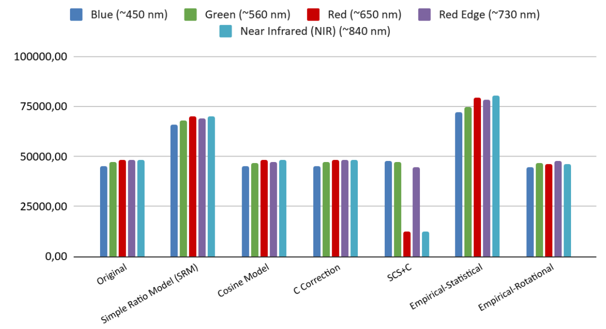

Figure 4. Median of calibration panels by model and band.

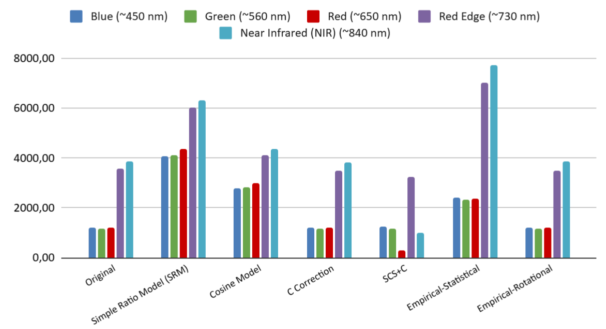

Figure 5. Standard deviation of calibration panels by model and band.

4. Discussion

The evaluation of the correction models revealed distinct performances depending on the spectral band and the statistical metric employed. Among the tested approaches, SCS+C and C Correction consistently demonstrated superior results, whereas SRM and Empirical-Statistical systematically increased reflectance values and variability among panels.
The SCS+C model showed particularly strong performance in the Red and NIR bands, which are the most sensitive to topographic effects and are widely used in vegetation monitoring through indices such as NDVI. The marked reduction in variability in these bands reinforces the suitability of SCS+C for UAV-based applications focused on vegetation and biomass monitoring, where radiometric consistency is crucial.
The C Correction model, although providing more moderate improvements, presented stable results across all spectral bands and did not introduce radiometric artifacts. This robustness, widely reported in orbital applications, makes C Correction a reliable choice for operational scenarios where consistency and reproducibility are more important than maximum variability reduction.
On the other hand, SRM and Empirical-Statistical frequently overcorrected reflectance values, increasing dispersion among panels. This effect is likely related to the high spatial resolution of UAV data, where small topographic variations produce large contrasts in illumination. These findings confirm that these models are not ideal for complex terrain conditions in low-altitude UAV imagery.
An important observation concerns the Green band, where none of the correction models provided a clear improvement over the uncorrected image. This result may be associated with the lower sensitivity of this band to topographic illumination effects, as vegetation reflectance in the green range is dominated by strong chlorophyll absorption and a relatively narrow dynamic range. In such cases, applying topographic corrections may introduce additional noise rather than improving radiometric consistency, and their use should be carefully evaluated.
Overall, these results highlight that topographic corrections originally developed for satellite imagery can be adapted to UAV data, but their performance is model- and band-dependent. The evidence supports prioritizing SCS+C when strong variability reduction is required, and C Correction when seeking a robust and conservative adjustment.

5. Conclusion

This study evaluated six classical and empirical topographic correction models applied to high-resolution multispectral imagery acquired by a UAV. The results demonstrated that the effectiveness of the models varied across spectral bands. SCS+C was the most effective correction method, especially in the Red and NIR bands, achieving substantial reductions in variability among calibration panels. C Correction provided consistent and stable improvements across all bands, confirming its robustness for operational applications.

In contrast, SRM and Empirical-Statistical consistently increased reflectance values and variability, confirming their limited suitability for UAV-based applications in areas of irregular terrain. The Green band results suggest that topographic corrections may not always be beneficial, as this band showed little sensitivity to illumination geometry.
By improving radiometric stability, effective corrections such as SCS+C and C Correction enhance the reliability of vegetation indices, biomass estimation, and environmental assessments. Future research should include additional datasets acquired under different illumination conditions and terrain configurations, explore the coefficient of variation as an alternative metric, and assess the impact of corrections on classification accuracy and change detection.

Acknowledgements

This study was supported by the National Council for Scientific and Technological Development (CNPq, Grant No. 308747/2021-6) and by the São Paulo Research Foundation (FAPESP, Grant No. 2021/06029-7). The authors gratefully acknowledge the support of the Department of Cartography of Universidade Estadual Paulista (FCT/UNESP) for providing the infrastructure and equipment necessary for data acquisition and processing.

References

Agisoft LLC. Agisoft Metashape Professional: version 2.2.1. St. Petersburg: Agisoft LLC, 2024. Available at: https://www.agisoft.com/. Accessed: 26 June 2025.

Blanco, P. D. et al., 2001. Topographic normalization in forest scenes. Remote Sens. Environ., 77(2), 128–137.

Cao, Y. et al., 2019. Topographic Correction Methods for UAV Multispectral Imagery. Remote Sens., 11(12), 2915.

Eisenbeiss, H. et al., 2004. UAV Photogrammetry for Topographic Mapping. Int. Arch. Photogramm. Remote Sens., XXXV-B5, 1–6.

ESRI. ArcGIS Pro: version 3.2. Redlands: Environmental Systems Research Institute, 2024. Available at: https://www.esri.com/en-us/arcgis/products/arcgis-pro. Accessed: 26 June 2025.

Ma, R. et al., 2013. Radiometric Correction in UAV Remote Sensing. ISPRS Annals, II-5/W2, 31–36.

Sellers, P., 1972. A formulation for atmospheric correction. Remote Sens. Environ., 2(3), 1–5.

Teillet, P. M. et al., 1982. An evaluation of topographic normalization techniques. Remote Sens. Environ., 13(2), 135–156.

Tan, Y. et al., 2010. Empirical Rotational Model for UAV-based imagery. Photogramm. Eng. Remote Sens., 76(5), 567–575.

Rosas, M. C. et al., 2020. Guidelines for UAV flights in topographic mapping. Rev. Bras. Cartogr., 72(3), 555–572.

Li, Z. et al., 2023. Evaluation of Topographic Correction Techniques for UAV Multispectral Images. Remote Sens., 15(8), 2059.